LEAD FREE METALLISATION PASTE FOR CRYSTALLINE SILICON SOLAR CELLS: FROM MODEL TO RESULTS

Jaap Hoornstra[1], Gunnar Schubert[2], Kees Broek[1],
Filip Granek[1], Cécile LePrince[3]
[1] ECN Solar Energy, PO Box 1, 1755 ZG Petten, the Netherlands
[2] University of Konstanz, PO Box X916, 78457 Konstanz, Germany
[3] Metalor Technologies, 45 Rue-de-Paris, 93130 Noisy-le-Sec, France

ABSTRACT

This work reports successful development of thick film lead free metallisation paste for contacting crystalline silicon solar cells. Models have been set-up to understand and describe the process of contact formation and current transport of front side metallisation pastes to silicon. New experimental test procedures have been developed to assess the models and minimize the number of experimental tests. The goal is to find in an intelligent way a replacement for the lead in the glass frit.

Using the outcome of this new contact model silver pastes with lead free glass frits have been formulated and tested using the new approaches. Cells were produced of Cz mono crystalline silicon material, with a 45 Ohm/square emitter and SiN_x antireflection coating. Using the best lead free silver front side pastes an efficiency of 16.6% was reached. This is equal to results from leaded reference pastes, and the best result published so far.

INTRODUCTION

For several years electronic industries have faced demands on working with environmentally clean materials. The new EU ROHS directive (restricted use of certain hazardous substances) requires that beginning July 2006, electrical and electronic equipment put on the market does not contain lead above a maximum concentration value of 0.1% by weight in homogeneous materials. At the moment this directive is not applicable to PV modules.

Currently in the PV world awareness exists in these matters, as is reflected by the work of Tsuo and de Wild [1,2]. In solar cell production several companies already anticipate these issues by advertising that lead free materials are used, accounting for e.g. lead free soldering or glass frit free rear side paste. In general however, pastes with lead containing glass frits are used to produce the electrical contacts. This European Commission granted project [3] was initiated to develop environmentally benign materials for crystalline silicon solar cells. The goal of the work reported here is to find a replacement for lead in glass frit and to produce competitive cell results with these lead free pastes compared to leaded pastes.

First reports on the unsuccessful use of lead free frits date from the seventies [4]. In the eighties, new attempts were reported [5] to use lead free frits; again not successful. This work reports the successful development of lead free pastes.

The work on contact formation modelling is described below, followed by the work on frit formulation. The final paragraph deals with experiments done to assess the performance of the developed frits and pastes on the cell level.

CONTACT FORMATION MODEL

Our approach for developing lead free front side pastes began with understanding the contact formation and current transport mechanism of successful lead containing silver pastes. We investigated competing processes separately and focused on the role of glass frit, especially on the role of lead oxide, in order to find a substitution for this metal oxide.

The contact formation was studied in detail using standard methods like SEM, EDX, DTA, and XRD. Additionally, new approaches such as in-situ contact resistance measurements have been used for this study [6]. Most of the experiments were performed in an RTP furnace, which provides accurate temperature control of the sample during firing. For maximum flexibility in the choice of constituents, glass frits were fabricated and their viscosity-temperature, wetting, and etching behaviour investigated.

It was found that the glass frit plays the most important role during contact formation. Its task is to etch through the antireflection coating and to ensure a stable mechanical contact. The glass also serves as a transport medium for silver to grow, preferably on <111> orientated silicon planes. It ensures the formation of nearly perfect silver–silicon contacts at temperatures below the silver–silicon eutectic. Various experiments with silver pastes and designed silver–glass–silicon systems were performed to study the silver transport and growth process in detail [6]. The results led to a detailed model of contact formation (see Fig. 1).

At temperatures typically above 600°C glass frit particles become fluid, wet the SiN_x, and start to etch. As soon as the glass has penetrated the dielectric layer, etching into silicon occurs via a redox reaction between lead oxide and silicon [7] (Fig. 1b). The resulting metallic

(a) (b) (c) (d) (e)

Fig. 1: Silver growth model. (a) Schematic cross section of Ag thick film paste on [100] silicon after burn-out. (b) Glass penetrated the dielectric layer → redox reaction between glass and silicon. (c) Silver particle dissolves in liquid lead. (d) Silicon interacts with liquid silver–lead alloy → formation of inverted pyramids. (e) Phase separation on cooling down → silver recrystallizes on <111> planes of the pyramid.

lead is liquid in this stage of the firing process. As soon as liquid lead comes into contact with silver, the particles melt to form a liquid silver–lead phase according to the Ag-Pb phase diagram (Fig. 1c). As simple experiments indicate, this process is very fast. The silver–lead melt is now in contact with the silicon surface. Dissolving of <100> silicon planes followed by inverted pyramid formation on <100> substrates starts at T > 700°C (Fig. 1d). On cooling down, silver and lead separate according to the phase diagram. Consequently silver re-crystallizes on the <111> planes of the inverted pyramids (Fig. 1e). Lead is therefore assumed to be the transport medium for silver to grow onto the silicon. The resulting microstructure was also confirmed by other authors [e.g. 8,9,10].

Although the dominant current transport mechanism in thick film silver contacts is not clearly established, silver crystallites seem to be indispensable for providing a current path from the emitter into the bulk of the thick film finger [8]. Most of the crystals are separated from the bulk of the silver finger by a glass layer; thus it is feasible that the glass frit also plays an important role for the current transport [11]. The tunnelling probability through the layer might be increased due to the chemical modification of the glass during the firing process.

LEAD FREE FRIT FORMULATION

Calculations were performed using the thermo-chemical software package FACTSAGE to evaluate which glass frit components could theoretically play an active role in the contact formation by forming molten metal particles in the firing process. First, a free Gibbs energy (ΔG) calculation scan was performed on a series of metal oxides to check if they are reduced by the SiN_x antireflection coating and by silicon during firing in air. Second, on the basis of these results a selection was made for so-called system calculations. Here ΔG was calculated for systems with more oxides present, like in a real frit, together with silver, SiN_x or Si, and air or argon. One of the assumptions in the calculation was that there was equilibrium at all temperatures. The physical behaviour of the components, like alloying with silver, was not taken into account. These calculations, combined with environmental considerations, resulted in only a few candidate oxides for replacing the lead oxide.

By following the contact formation model, it is essential for lead free glass to contain metal oxides that are reduced by silicon in the relevant temperature regime. The resulting metal forms an alloy with silver, interacting with silicon in a way that an almost perfect metal-semiconductor contact is formed. The etching rate of glass in silicon should be smaller than the etching rate in the antireflection coating, providing a wide process window.

These requirements led to the fabrication of several silicate glasses varying in metal oxide species and content. The essential frit properties, e.g. silicon wetting and etching, were tested and evaluated. Additionally, the silver transfer process was investigated.

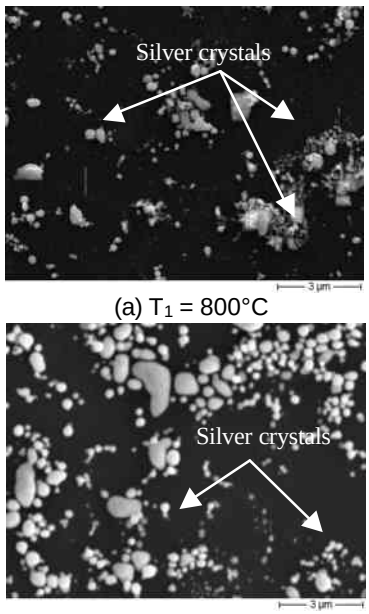

(a) T_1 = 800°C

(b) T_2 =850°C

Fig. 2: SEM photographs of <100> FZ, chemically polished silicon surfaces with a 38 Ohm/sq. emitter. Samples were fired at different peak temperatures in an RTP-furnace. After firing silver fingers were etched off. Silver crystals are clearly visible (white). Number and size of crystals increase with increasing temperature.

In Fig. 2 the temperature dependence of the silver transfer process of a lead free silver thick film paste is presented. The SEM pictures show the <100> orientated silicon surface after etching off the silver fingers successively in warm HCl (conc.) and HF (5%). Number and size of the silver crystals increase with increasing

temperature. The silver transfer process proved to be successful. It is shown that a lead free glass frit containing appropriate metal oxides can provide the key properties for establishing a good electrical contact to the emitter of a solar cell.

EXPERIMENTS: PASTES PERFORMANCE

Based on the results from the model, experiment results, and the thermo chemical calculations, several non-lead glass frits were formulated and used to make pastes with standard composition and rheology. These pastes were tested for performance and compared with commercial standard pastes using leaded frit. Cells were produced of 156 cm² square texturized Cz mono crystalline silicon material, with a 45 Ohm/square emitter and SiN_x antireflection coating and using a standard aluminium rear side paste.

Cells were processed using standard screen printing, drying and IR co-firing. Two cells per firing optimisation setting were processed and the cells were then analysed in detail. The primary goal was to see in a simple and efficient way if these pastes could provide an electrical contact, make a proper cell and achieve at least the performance set by the best reference paste.

When testing a paste, it is necessary to perform a firing optimisation step, where a variety of belt speed and zone set-temperatures are used to achieve maximum cell fill factor and efficiency while keeping the resistance losses as low as possible. To speed up the firing optimisation and decrease the number of tests the procedure using a non-flat cross belt temperature profile is used [12]. The approach is based on relating local contact resistance to local cell temperature. Spatially resolved wafer temperatures are measured as a function of relevant furnace settings using a Datapaq temperature profiler [13]. The Corescan instrument [14] is applied to map the contact resistance distribution. To significantly reduce the number of test trials, the approach uses a cross belt temperature gradient to fire a cell. This means that in one run, various locations on the cell are exposed to different temperatures. By relating the local contact resistance to the local wafer temperature, it is possible to assess if a paste leads to reasonable contact resistance values, and if so, the temperature setting for optimal firing can be easily established. In a final step, optimum firing is obtained and best cells are produced.

The best cells were characterized by IV, Suns-Voc FF [15], and on line resistance and contact resistance.
IV: IV data were measured at ECN with a class A solar simulator using two probes per bus bar.
Suns-Voc: From the Suns-Voc measurement we obtain the series resistance-less fill factor. If this value is around 80% in our case, we assume no shunting of the emitter or no damage to the junction occurred due to metallisation. The difference between IV FF and Sinton-Voc FF is a measure for the actual series resistance.
Busbar-busbar resistance: Used to measure the average finger resistance.
Corescan: Mapping of the local contact resistance, often the limiting factor in paste performance.

The contacts of selected cells were analysed using SEM. Etching performance of the glass frit through the SiN_x coating, plus growth rate of silver crystallites on the silicon surface were measured. In addition, the influence of a forming gas anneal (FGA) treatment on the contacts formed was assessed by exposing a selection of cells to a forming gas of an H_2/Ar mixture at 400°C for 15 minutes.

RESULTS AND DISCUSSION

The Datapaq was used to map the actual wafer temperatures in case of non-flat cross belt temperature profiles and standard flat cross belt profiles. In Fig. 3 the actual wafer temperatures, as measured in the centre of a wafer with SiN_x coating and with the test wafer in the middle of the belt, are given as a function of relative belt speed and peak zone temperature settings for the setting domain used. These iso-temperature lines were helpful in setting the furnace and for choosing relevant settings for the non-flat cross belt approach mentioned before.

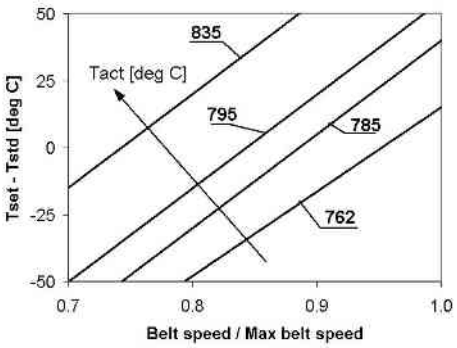

Fig. 3: Actual wafer temperatures as a function of furnace settings.

As an example of the non-flat cross belt approach, Fig. 4 shows a compilation of Corescan mappings for a lead free paste as function of wafer temperature. Corescan pictures for three non-flat cross belt settings have been used together with the local wafer temperatures. The paste reaches minimum contact resistance at T_{act} ~ 835°C. This is about 25 degrees higher than for the reference paste.

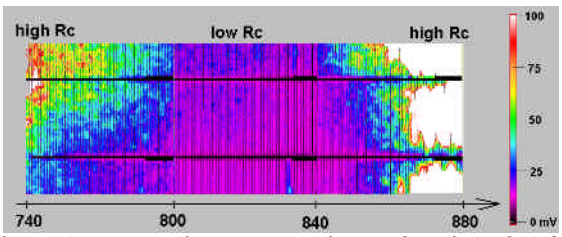

Fig. 4: Contact resistance mapping as function of wafer temperature. Temperature scale is not linear.

Based on the results from the non-flat cross belt temperature testing, selected pastes have been used to

make cells using the standard (i.e. flat) cross belt temperature distribution.

Fig. 6 gives the evolution of best FF results of the series experiments using various lead free frits, and shows by the improvement of FF the realisation of good electrical contacts.

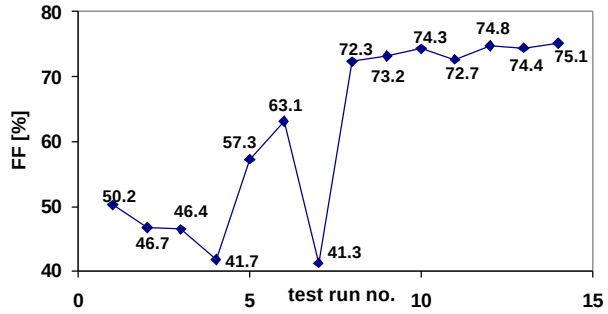

Fig. 6: Evolution of best FF results for test runs with different frits, pastes and using different settings.

The best cell results, together with Suns-Voc FF and line resistance values of reference and lead free pastes are given in table 1. The IV results were corrected for spectral mismatch. The results show that with the lead free paste equivalent efficiency and fill factor are reached, as compared to the leaded reference paste. The relatively low FF values reflect the use of two probes per busbar.

Paste	IV FF [%]	Suns-Voc FF[%]	eta [%]	Jsc [mA/cm^2]	Voc [mV]	R_L [Ω/cm]
Reference	75.3	81.3	16.5	35.6	618	0.280
Lead Free	75.1	81.0	16.6	35.9	616	0.221

Table 1: Best cell results for leaded reference and lead free silver paste.

In order to study if FGA treatment would further improve the cell results, a selection of 10 lead free cells received FGA treatment. Overall, cell performance was improved. The fill factor for the best cells increased up to 0.2% abs. For cells with initial FF in the range of 71-73%, the improvement was up to 2.5% abs., increasing the firing window and process yield effectively.

The previously described approach has demonstrated to work well for the optimisation of frits and evaluation of pastes. Current testing has shown that we have achieved equivalent contact performance results when compared to the leaded paste. Final tuning of the paste composition and rheology, and front side pattern parameters can lead to further improvements in performance of lead free pastes.

CONCLUSIONS

A model has been developed to describe the formation of the thick film silver contact and has been supported by detailed analysis and characterization. The roles of lead oxide and silver have been established. Using the model and associated thermo dynamical calculations, lead free glass frits have been formulated.

Pastes with these frits have been successfully tested using a fast approach for firing optimisation and characterisation. The best lead free frit formulation resulted in cells with same efficiency (16.6%) and fill factor (75.1%) as for the leaded reference paste. With these first and best results ever published, lead free paste has been successfully developed.

REFERENCES

[1] Y.S. Tsuo et al, July 1998, NREL/CP-590-23901

[2] M.J. de Wild-Scholten et al, REFOCUS 5 (5), 2004, 46-49

[3] EC FP5 program EC2Contact project (#ENK6-CT-2001-00560)

[4] S. Hogan et al, SERI report TR-611-1186, 1981

[5] R. Mertens et al, *17th IEEE*, 1984, 1347-1351

[6] G. Schubert et al, *19th EPVSEC*, Paris, 2004, 813-816

[7] G. Schubert et al, *PV in Europe Conference*, Rome, 2002, 343-346

[8] C. Ballif et al, *Appl. Phys. Lett.* **82**, No. 12, 2003, 1878-1880

[9] C. Khadilkar et al, *14th PVSEC*, Bangkok, 2004 in print

[10] M.M. Hilali et al, *19th EPVSEC*, Paris, 2004, 1300-1303

[11] G. Schubert et al, *14th PVSEC*, Bangkok, 2004, in print

[12] J. Hoornstra et al, *19th EPVSEC*, Paris, 2004 1044-1047

[13] Furnace temperature profiler: www.datapaq.com

[14] A.S.H. van der Heide et al, *Solar Energy Materials and Solar Cells* **74,** 2002, p.43

[15] R.A. Sinton, *9th NREL Workshop on Crystalline Silicon Solar Cell Mat. and Processes*, 1999, 67-73

ACKNOWLEDGEMENTS

This work was supported by the EC in the frame of the FP5 program within the EC2Contact project (#ENK6-CT-2001-00560). Partner RWE Schott Solar is acknowledged for the cell material.